

Phonon-induced decay of a quantum-well hole: One monolayer Na on Cu(111)

B. Hellsing, J. Carlsson, L. Walldén, and S.-Å. Lindgren

Department of Physics, Chalmers University of Technology and Göteborg University, S-412 96 Göteborg, Sweden

(Received 14 September 1999)

The phonon-induced decay of an overlayer quantum-well hole is investigated theoretically and considered for one monolayer of Na on Cu(111). The electron-phonon coupling matrix element is determined by a *first-principles* deformation potential and model potential wave functions. The main contribution to the lifetime broadening can be attributed to the electron-phonon coupling in the overlayer and interface region. Peak width and temperature dependence are consistent with photoemission data.

The characterization of nanoscale confined systems with quantum size effects is currently of great interest. This is due to the rapid development of experimental techniques for tracing quantum effects in, e.g., electric conductance and surface reactivity as well as the obvious interest from the microelectronic industry. Quantization of electric conductance has been observed in narrow constrictions, with diameters of a conduction-electron wavelength,¹ and in semiconductor devices containing a two-dimensional electron gas.²⁻⁴ Recent experiments have demonstrated the possibility of controlling chemical reactions by manipulating the size of adsorbed ultrathin metal islands.^{5,6} The dynamics of these phenomena involve elastic and inelastic electron scattering, which determine the relaxation time in conductivity and lifetimes of key electronic excitations promoting specific chemical reactions. The finite lifetime is due to electron-electron and electron-phonon interactions. The electron-electron interaction has been shown to play an important role in the decay of surface image states.⁷ Ultrathin layers adsorbed on metal surfaces form well-defined model systems appropriate for studies of relaxation dynamics of quantum states.^{8,9} The quantum-well states, formed in the overlayer due to a local band gap in the metal substrate, have been monitored and analyzed accurately⁸ with angular-resolved photoemission electron spectroscopy (ARPES).^{10,11}

Information about quantum-well dynamics can be obtained from line-shape analysis of photoemission spectra. The peak width yields lifetime information of the photoinduced excitation. A recent interferometric time-resolved two-photon photoemission technique is promising for a direct determination of excitation lifetimes.^{12,13} The technique has been applied to determine the lifetime of the hole formed when removing an electron from the Cu(111) *sp*-surface state.¹² The results clearly indicate that the lifetime broadening accounts for the observed peak width in ARPES.¹⁴ We expect that in the case of a surface state, as well as for an overlayer quantum-well state, the finite lifetime of the emitted electron reduces the peak intensity due to a limited escape depth,¹⁵ and no broadening is introduced due to the uncertainty of the normal momentum.¹⁶ This means that the intrinsic linewidth represents the lifetime broadening of the hole state.

Photoemission studies of the Cu(111) *sp*-derived surface state have been presented, focusing on the temperature dependence of the peak width.^{17,14} Matzdorf, Meister, and

Goldmann¹⁷ pointed out that the temperature dependence is not consistent with a Debye-Waller effect and McDougall, Balasubramanian, and Jensen¹⁴ suggested that the linear temperature dependence of the width in the temperature range $30 \text{ K} \leq T \leq 625 \text{ K}$ is consistent with an electron-phonon coupling mechanism. The argument is based on the theoretical high-temperature result for the width $2\pi\lambda(\vec{k})k_B T$, which is the phonon-induced lifetime broadening of a state with an energy $\epsilon(\vec{k})$ close to the Fermi energy in bulk metals.^{18,19} The mass enhancement factor $\lambda = 0.14$, deduced from the experiment using the above formula, agrees reasonably well with bulk calculations by Khan *et al.*²⁰ and cyclotron masses deduced by Lee.¹⁸ The interpretation in terms of electron-phonon interaction is reasonable. However, a more detailed theoretical investigation is required for the analysis of the experimental data. In comparison with bulk states, the surface state is two-dimensional (2D)-like, which introduces phase-space restrictions. Furthermore, the phonon-assisted electron scattering into the hole will only take place from electron states with an appreciable amplitude in the surface region in order to yield a significant contribution to the electron-phonon matrix element.

Recently, a line-shape analysis of the photoemission spectra has been presented for the system of one monolayer of Na adsorbed on Cu(111).⁸ The near Lorentzian shape of the quantum-well peak indicates a lifetime broadening, and furthermore, the width increased linearly with temperature in the range $130 \text{ K} \leq T \leq 295 \text{ K}$. According to electron-gas theory,²¹ the broadening due to electron-electron scattering ($\approx 1 \text{ meV}$) is much smaller than the experimentally observed width [$\approx 50 \text{ meV}$ (Ref. 8)], which suggests that the lifetime broadening has a substantial contribution due to the electron-phonon coupling.

With this background, we estimate the lifetime broadening due to the electron-phonon coupling and then compare with experiments for the system 1-ML Na on Cu(111). The renormalization of the one-electron state due to the creation of the hole can be expressed in terms of the self-energy. We focus on the imaginary part of the self-energy, which is half the full width at half maximum (FWHM), Δ_1 , of the lifetime broadening.

The self-energy of a hole state introduced when an electron is removed, $N \rightarrow N-1$, is derived similarly to the complementary case when an extra electron is added, N

$\rightarrow N+1$.¹⁹ To meet the experimental conditions, we consider the case of an ejected quantum-well electron with no parallel momentum. The contribution to Δ_1 due to the interaction between the electrons and the phonons within the overlayer of frequency $\Omega_{\vec{q}_{\parallel}}$ and polarization $\vec{\epsilon}$ is determined to the lowest order by the expression

$$\begin{aligned} \Delta_1 = & 2\pi \sum_{n, \vec{k}_{\parallel}} |g_{n, \vec{k}_{\parallel}}|^2 \{ [f(E_{n, \vec{k}_{\parallel}}) + n_B(\Omega_{\vec{q}_{\parallel}})] \\ & \times \delta(\epsilon_0 - E_{n, \vec{k}_{\parallel}} + \hbar\Omega_{\vec{q}_{\parallel}}) + [1 + n_B(\Omega_{\vec{q}_{\parallel}}) - f(E_{n, \vec{k}_{\parallel}})] \\ & \times \delta(\epsilon_0 - E_{n, \vec{k}_{\parallel}} - \hbar\Omega_{\vec{q}_{\parallel}}) \}, \end{aligned} \quad (1)$$

where $n_B(\Omega_{\vec{q}_{\parallel}})$ and $f(E_{n, \vec{k}_{\parallel}})$ are the phonon and electron occupation numbers, and ϵ_0 is the renormalized hole energy at the $\bar{\Gamma}$ point. The summation is over all one-electron states with band index n and momentum \vec{k}_{\parallel} parallel to the surface. Momentum conservation requires $\vec{q}_{\parallel} + \vec{k}_{\parallel} = 0$. The electron-phonon coupling constant $g_{n, \vec{k}_{\parallel}}$ is given by the expression¹⁹

$$g_{n, \vec{k}_{\parallel}} = \sqrt{\frac{\hbar}{2MN\Omega_{\vec{q}_{\parallel}}}} \langle \Phi_{0,0} | \vec{\epsilon} \cdot \vec{\nabla}_{\vec{R}} V_e | \Phi_{n, \vec{k}_{\parallel}} \rangle_0, \quad (2)$$

where N is the number of overlayer ions, M is the effective mass of the adsorbate ion, and \vec{R} is the nuclear displacement of a single adsorbate ion from the equilibrium position. The lower index “0” to the right of the ket vector denotes evaluation at the equilibrium position. V_e is the effective one-electron potential, and $\Phi_{n, \vec{k}_{\parallel}}$ and $\Phi_{0,0}$ are the initial and final one-electron states, respectively. Band index $n=0$ denotes the band of the hole state. The first term in the curly brackets in Eq. (1) corresponds to phonon emission and the second to phonon absorption. To obtain the net scattering rate of electrons into the hole state, we have, in the square brackets of Eq. (1), taken into account the process when an electron is scattered out of the hole state either by absorbing a phonon (in the first term) or by emitting a phonon (in the second term).

The phonon and electron states are modeled as follows. According to helium-atom scattering (HAS) experiments on the system 1-ML Na on Cu(100),²² the phonon dispersion is flat, referring to the phonon energy versus parallel momentum \vec{q}_{\parallel} . Furthermore, the observed vibrational modes are consistent with “organ pipe” type of modes normal to the surface.²² The large HAS intensities recorded are interpreted by Benedek *et al.* as an indication that the overlayer vibrational displacements are normal to the surface, e.g., the polarization is in the z direction.²² Assuming the conditions are similar for 1 ML of Na on Cu(111), the flat dispersion suggests that an Einstein model for the overlayer vibrational mode polarized normal to the surface is reasonable. The energy of the single mode is denoted $\hbar\Omega_0$. In principle, the copper bulk phonons contribute since the overlayer vibrational energy is right in in the bulk phonon band. However, our aim is to study the contribution from the overlayer vibrations, which should be significant due to the localization of

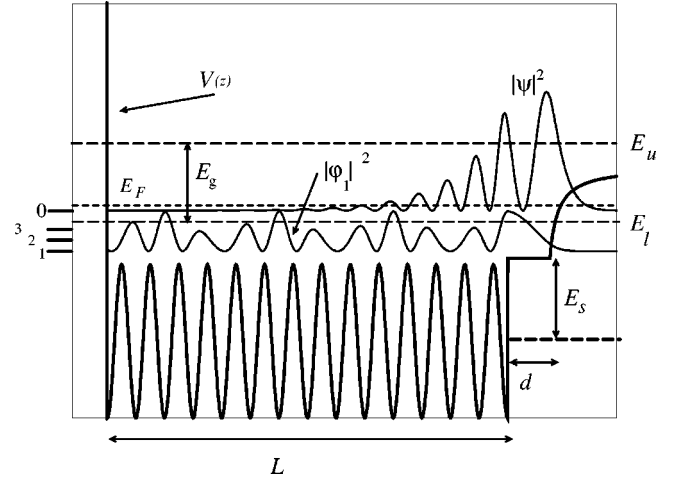


FIG. 1. Model potential V (thick solid line) and wave functions absolute squared in the direction of the surface normal for a slab with thickness of 14 Cu layers and a full monolayer of Na atoms. $z=0$ is located half a Cu interlayer distance (1.04 Å) outside the outermost copper layer, ψ the quantum-well wave function, and ϕ_1 the wave function of the lowest-energy resonance states. The resonance states are the bound states in the energy range $E_s \leq E \leq E_l$. The eigenenergies at the $\bar{\Gamma}$ point are indicated to the left by horizontal bars; one quantum-well state ϵ_0 and three resonance states $\epsilon_1, \epsilon_2, \epsilon_3$. The overlayer thickness, $d=3.07$ Å (Ref. 25) and Na overlayer energy step $E_s=5.4$ eV (Ref. 25). The Cu band gap in the $\langle 111 \rangle$ direction is given by $E_g=E_u-E_l=5$ eV, where E_u and E_l are the upper and lower band-gap edges at the L point of the Cu Brillouin zone, respectively.

the quantum-well wave function. Comparing the results of experiments and our calculations below indicate that our expectation seems correct.

The two types of electron states that have an appreciable amplitude in the overlayer region are written as

$$\Phi_{0, \vec{k}_{\parallel}}(z, \vec{x}) = \frac{1}{\sqrt{\Omega}} \psi(z) e^{i\vec{k}_{\parallel} \cdot \vec{x}}, \quad E_{0, \vec{k}_{\parallel}} = \epsilon_0 + \hbar^2 k_{\parallel}^2 / 2m^*, \quad (3)$$

$$\begin{aligned} \Phi_{n, \vec{k}_{\parallel}}(z, \vec{x}) &= \frac{1}{\sqrt{\Omega}} \phi_n(z) e^{i\vec{k}_{\parallel} \cdot \vec{x}}, \quad E_{n, \vec{k}_{\parallel}} = \epsilon_n + \hbar^2 k_{\parallel}^2 / 2m, \\ n &= 1, 2, \dots, N_L, \end{aligned} \quad (4)$$

where $\Phi_{0, \vec{k}_{\parallel}}$ are the quantum-well states, and $\Phi_{n, \vec{k}_{\parallel}}$, $n=1, 2, \dots, N_L$, are the states located in the energy range $E_s \leq E \leq E_l$, which are denoted resonance states (see Fig. 1). m^* and m are the electron masses parallel to the surface for the quantum-well state and the resonance states, respectively, z and \vec{x} denote the coordinate normal and parallel to the surface, N_L is the number of resonance states, which is determined by the thickness L of the copper slab, and Ω denotes the surface area of the Na overlayer. ψ and ϕ_n are obtained by matching the analytical solutions of the Schrödinger equation for the one-dimensional model potential V , which is shown for the case $L=13.5$ Å in Fig. 1.

V has three parts: (i) the copper part, $V=V_0-2V_g \cos(gz)$ for $-L \leq z \leq 0$; (ii) the Na overlayer, $V=E_s$

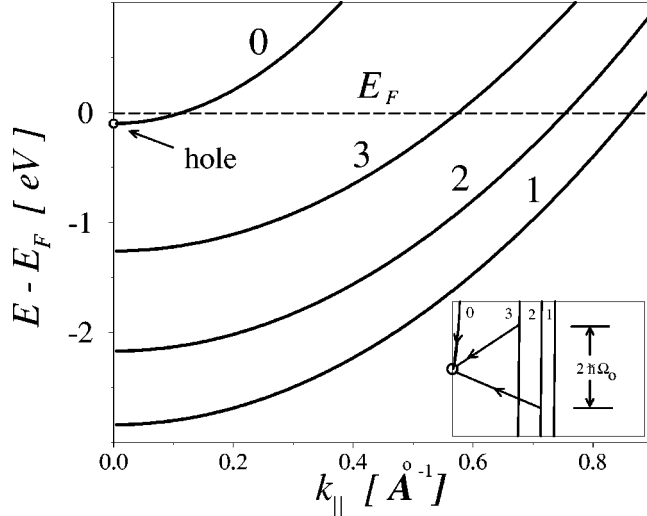


FIG. 2. Free-electron-like bands in the direction parallel to the surface. The bands that represent the states shown in Fig. 1 are drawn with an effective electron mass of $0.5m_e$ for the quantum-well state and with the free-electron mass m_e for the resonance states (1,2,3). In the inset a blow-up is shown to illustrate three of the seven possible phonon-assisted transitions that can take place: $0 \rightarrow \text{hole}$ represents the intraband scattering including phonon emission while $3 \rightarrow \text{hole}$ and $2 \rightarrow \text{hole}$ represent interband scattering including phonon emission and absorption, respectively.

for $0 < z \leq d$; and (iii) the image potential for $z > d$. $2V_g$ and g are the band-gap energy and the shortest reciprocal-lattice vector in the $\langle 111 \rangle$ direction, respectively. For the potential in the Na overlayer and the position of the image plane z_{im} , we use the values given by Lindgren and Walldén,²³ $E_s = 5.4$ eV, $d = 3.07$ Å, and $z_{\text{im}} = 2.46$ Å (see Fig. 1). For states appearing in the local band gap in the $\langle 111 \rangle$ direction, $2V_g \equiv E_g = E_u - E_l = 5$ eV, the nearly free-electron (NFE) model for copper yields an exponentially damped oscillatory form of ψ into the copper crystal²⁴ (see Fig. 1). E_u and E_l denote the energy of the upper and lower band-gap edge at the L point of the copper Brillouin zone, respectively. One single quantum-well state appears as a solution, when a total phase shift for a round trip in the overlayer of an integer number times 2π is required.²³ The resonance states ϕ_n are Bloch states in the copper crystal and are also determined within the NFE approximation.

We would like to make two remarks at this point. First, the model potential presented in Fig. 1 is given for specific values of the overlayer parameter E_s and d . These values are determined in order to reproduce the experimentally determined energy of the quantum-well state (0.1 eV below E_F). A recent *first-principles* calculation²⁵ also shows that the shape of the quantum-well wave function ψ is very well described by the wave function deduced from the model potential in Fig. 1. These facts strengthen our confidence in using wave functions determined by the model potential when calculating the electron-phonon matrix elements in Eq. (2). Second, we want to point out that in the actual calculation of Δ_1 , according to Eq. (1), the thickness of the copper slab has to be extended further in comparison with the one given in Fig. 1 in order for the expression in Eq. (1) to converge.

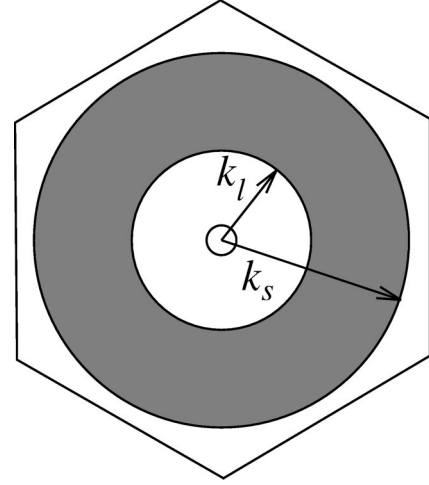


FIG. 3. The 2D overlayer Brillouin zone. The small inner circle, with radius $\sqrt{2m^*\Omega_0/\hbar}$, corresponds to the line of integration for the intraband scattering. The shaded area shows the region of integration for the interband scattering. The minimum and maximum radii, denoted k_l and k_s , are given by $k_l = \sqrt{2m(\epsilon_0 - \hbar\Omega_0 - E_l)}/\hbar$ and $k_s = \sqrt{2m(\epsilon_0 + \hbar\Omega_0 - E_s)}/\hbar$. The values of the parameters m^* , m , E_l , and E_s are given in Figs. 1 and 2.

The electron-phonon coupling includes intraband and interband scattering, referring to the free-electron-like subbands parallel to the surface (these transitions are illustrated in the inset of Fig. 2). In the case of intraband scattering, only phonon emission is possible, while interband transitions include both phonon absorption and emission. The intraband and interband scattering involve \vec{k} -space integrations over the inner circle and the shaded area in Fig. 3, respectively. Equations (1)–(4) yield the following result

$$\Delta_1 = \frac{1}{2n_a\hbar\Omega_0} \left[\zeta^{\text{intra}}(T) \frac{m^*}{M} |G_0 M_0|^2 + \zeta^{\text{inter}}(T) \frac{m}{M} \sum_{n=1}^{N_L} |G_n M_n|^2 \right]. \quad (5)$$

The first and second term in the square brackets refer to intraband and interband scattering, respectively. The temperature dependence is given by the functions

$$\zeta^{\text{intra}}(T) = f(\epsilon_0 + \hbar\Omega_0) + n_B(\Omega_0) \quad (6)$$

and

$$\zeta^{\text{inter}}(T) = \coth\left(\frac{\hbar\Omega_0}{2k_B T}\right) + \frac{1}{2} \left[\tanh\left(\frac{\epsilon_0 - E_F - \hbar\Omega_0}{2k_B T}\right) - \tanh\left(\frac{\epsilon_0 - E_F + \hbar\Omega_0}{2k_B T}\right) \right]. \quad (7)$$

In Eq. (5), $\hbar\Omega_0$ is the energy of the overlayer Einstein vibrational mode, and n_a is the surface density of Na atoms ($n_a = 0.086$ Å⁻²). The electron-phonon matrix element corresponding to intraband and interband scattering at a single Na atom site is given by $M_0 = \langle \psi | \partial V_e / \partial R_z | \psi \rangle_0$ and $M_n = \langle \psi | \partial V_e / \partial R_z | \phi_n \rangle_0$, respectively. $G_n = n_a \int_{\Omega_{\text{WS}}} e^{i\vec{k} \cdot \vec{x}} d\vec{x}$

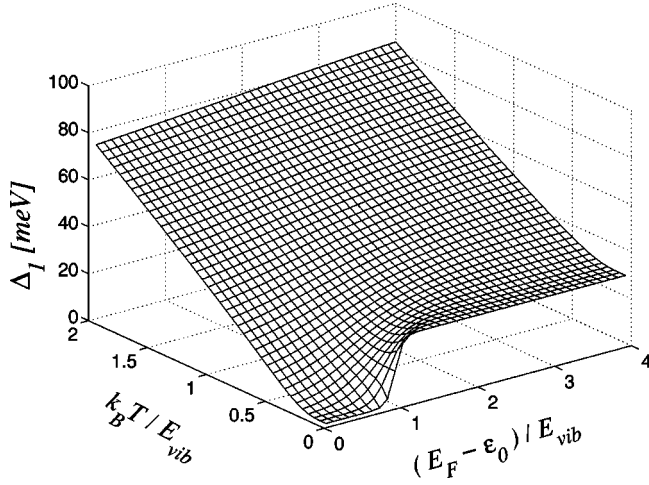


FIG. 4. 3D plot of the calculated width Δ_1 [Eq. (5)] vs temperature and binding energy in units of the vibrational energy $E_{\text{vib}} = \hbar\Omega_0 = 21$ meV.

$= 2\pi n_a k_n^{-2} \int_0^{\xi_n} \xi J_0(\xi) d\xi$ are dimensionless shape factors with $\xi_n = k_n R_{\text{WS}}$, where $R_{\text{WS}} = 1.83 \text{ \AA}$ is the Wigner-Seitz radius of the Na atom and $k_0 = \sqrt{2m\Omega_0}/\hbar$, and for $1 \leq n \leq N_L$, we have $k_n = \sqrt{2m(\epsilon_0 - \epsilon_n)}/\hbar$ as $\epsilon_0 - \epsilon_n \gg \hbar\Omega_0$ (see Fig. 1).

In the calculations we model the semi-infinite copper bulk by taking the limit $L \rightarrow \infty$, which makes the sum in Eq. (5) formally converge. In practice it is sufficient to have $L \approx 120 \text{ \AA}$, which yields eight resonance states.

From Eqs. (6) and (7), we easily obtain the linear temperature coefficient at high temperatures ($k_B T \gg \hbar\Omega_0$),

$$\Delta_1 = \gamma T, \quad (8)$$

where

$$\gamma = \frac{k_B}{2n_a} \left(\frac{m^*}{M} \left| \frac{G_0 M_0}{\hbar\Omega_0} \right|^2 + 2 \frac{m}{M} \sum_{n=1}^{N_L} \left| \frac{G_n M_n}{\hbar\Omega_0} \right|^2 \right). \quad (9)$$

Analyzing Eqs. (5)–(9), we find that the fingerprint of the electron-phonon mechanism for hole decay is the characteristic behavior in the temperature range $0 \leq k_B T \leq \hbar\Omega_0$ and hole energy range $0 \leq E_F - \epsilon_0 \leq 2\hbar\Omega_0$.

In the 3D plot in Fig. 4, the quantitative temperature and binding-energy dependence of Δ_1 is shown. If the hole is within $\hbar\Omega_0$ of the Fermi level, $\Delta_1 \rightarrow 0$ as $T \rightarrow 0$. The lack of electrons above the Fermi level prevents both intraband and interband scattering, including phonon emission. Furthermore, interband scattering due to phonon absorption is suppressed as no phonons are present at $T=0$. On the other hand, if the hole energy is more than $\hbar\Omega_0$ below the Fermi level, a nonzero value is obtained $\Delta_1 \rightarrow \gamma \hbar\Omega_0 / 2k_B (2\gamma_{\text{intra}} + \gamma_{\text{inter}})$ as $T \rightarrow 0$ as in this case both intraband and interband scattering which involve phonon emission can take place even at $T=0$. γ_{intra} and γ_{inter} represent the two contributions to γ from left to right in Eq. (9).

The contribution to the experimental width due to the finite hole lifetime, introduced by the electron-phonon coupling, is determined by Δ_1 in Eq. (5). Important quantities for a theoretical estimate of Δ_1 are the deformation potential

$\partial V_e / \partial R_z$ and the vibrational energy $\hbar\Omega_0$. To obtain a reasonable estimate of the electron-phonon coupling, we use a deformation potential of *ab initio* quality. This is needed since both the length scale and the strength of the dynamic screening is in general nonsymmetric with respect to the adsorbate layer due to the inhomogeneous electron density at the surface. We evaluate the deformation potential and the vibrational energy from a *first-principles* density-functional theory (DFT) calculation^{26,27} using the generalized gradient approximation for the exchange-correlation functional,²⁸ applying a plane-wave basis and ultrasoft pseudopotentials²⁹ for both Na and Cu. The DACAPO code was used in the calculation.^{30,31}

The deformation potential is calculated as $\partial V_e / \partial R_z \approx [V_{\text{DFT}}(R_z = \delta Q) - V_{\text{DFT}}(R_z = 0)] / \delta Q \equiv (\delta V_e / \delta Q)_{\text{DFT}}$. $V_{\text{DFT}}(R_z = 0)$ and $V_{\text{DFT}}(R_z = \delta Q)$ are the z -dependent self-consistent effective one-electron potential, averaged parallel to the surface over the unit cell, when the Na monolayer is in the relaxed equilibrium ground state and when it has been rigidly displaced $\delta Q = 0.1 \text{ \AA}$ in the normal direction away from the copper substrate, respectively. The copper substrate ion positions are kept fixed when the Na overlayer is displaced. For this system this rigid substrate approximation is reasonable, which will be discussed further below. We apply the electron wave functions derived from the model potential (Fig. 1) evaluating the matrix elements $M_0 = \langle \psi | (\delta V_e / \delta Q)_{\text{DFT}} | \psi \rangle_0$ and $M_n = \langle \psi | (\delta V_e / \delta Q)_{\text{DFT}} | \phi_n \rangle_0$ for the intraband and interband scattering, respectively.

For a rigid substrate lattice, a vibrational energy $\hbar\Omega_0 = 21$ meV is obtained from the curvature of the total energy with respect to the Na layer displacement. An upper limit for the substrate lattice-dynamic influence has been estimated by letting the copper substrate ions fully relax their positions after the Na layer has been displaced a typical vibrational amplitude and held rigidly in their displaced positions. This resulted in a slightly softer total energy parabola corresponding to a small down shift of the vibrational energy of 3 meV (from 21 to 18 meV).²⁵ An upper limit of 3 meV for the down shift of the vibrational energy suggests that the copper ions of the Cu(111) surface are more or less rigid considering the ground and first excited state of this vibrational mode, which in turn implies that the effective adsorbate mass M is approximately given by the free sodium-atom mass.

Referring to experiment, the calculated vibrational energy is reasonable. For Na on Cu(111) the vibrational energy has only been measured in the coverage range 0–0.35 ML and found to be almost constant ~ 21 meV.³² Experimental data are available for 1-ML Na on Cu(100), and in this case the vibrational energy is $\hbar\Omega_0 = 18$ meV.²²

The experimentally observed width Δ is considered to have contributions from inhomogeneous broadening Δ_0 and homogeneous broadening Δ_1 . If the inhomogeneous energy broadening is represented by a Lorentzian distribution, the convolution of the Lorentzian describing the phonon-induced lifetime broadening yields

$$\Delta = \Delta_0 + \Delta_1. \quad (10)$$

From the calculations, we find approximately equal contribution from interband and intraband scattering. We have one adjustable parameter, the inhomogeneous broadening

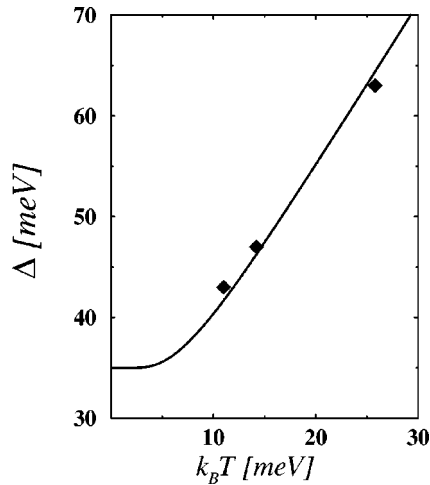


FIG. 5. The FWHM width vs the thermal energy $k_B T$. The solid line represents the temperature dependence of $\Delta = \Delta_0 + \Delta_1$, when Δ_1 is obtained from Eq. (5) with the calculated vibrational energy $\hbar\Omega_0 = 21$ meV. $\Delta_0 = 6$ meV is determined by a least-squares fit to the three experimental points (Ref. 8) (diamonds).

Δ_0 , essentially determined by the quality of the sample, the amount of impurities and defects. A least-squares fit to the three experimentally observed widths (see Fig. 5) yields $\Delta_0 = 6$ meV for a rigid substrate lattice ($\hbar\Omega_0 = 21$ meV). The calculated zero-temperature lifetime contribution to the width is 29 meV. In Fig. 5 we show the best fit of the parameter Δ_0 to match the experimental data. It is striking how well our relatively simple model calculation reproduces the experimental observations.

The high-temperature linear coefficient γ [Eq. (9)] is calculated to be 0.16 meV/K. Now, in order to obtain some understanding of the strength of the electron-phonon coupling, we compare with copper bulk results. γ is related to a ‘‘mass enhancement factor’’ λ by the relation $\gamma = 2\pi k_B \lambda$. With λ values reported for the neck orbit of bulk copper perpendicular to $\langle 111 \rangle$, $\lambda = 0.16$ (Ref. 20) and $\lambda = 0.23$,¹⁸ we obtain $\gamma = 0.09$ meV/K and $\gamma = 0.12$ meV/K, respectively. These values are smaller than what we calculate for the quantum-well state (0.16 meV/K), which seems surprising as the \vec{k} space of integration is considerably reduced in comparison with the copper bulk Fermi-surface area. We want to point out that the gamma value $\gamma = 0.12$ meV/K deduced from experiment in a previous study⁸ is in the light of the

present work not a saturated high-temperature value. An additional 30% increase is expected if measurements were possible at still higher temperatures.

γ crucially depends on the phase-space integration and the electron-phonon coupling matrix elements. It is well known that the electron-phonon coupling differs in the inhomogeneous electron gas at the surface compared with, say, a homogeneous density corresponding to the average surface electron density. At the surface the charge-transfer mechanism is expected to completely dominate the potential scattering mechanism, which dominates in the bulk.³³

To summarize, we present a simple model aimed to focus on the important parameters that determine the lifetime broadening of quantum-well states due to the electron-phonon coupling in metallic adlayers on metals. Simple formulas for the lifetime broadening and the linear temperature coefficient γ are obtained. The low-temperature behavior of the lifetime broadening is predicted and gives qualitatively different results depending on the hole binding energy versus vibrational energy. In the context of electron-phonon coupling at surfaces, this theoretical analysis illustrates how the electron-phonon matrix elements in the surface region more than compensate for the limited phase space.

In the calculations of the electron-phonon coupling matrix elements $\langle f | \delta V | i \rangle$, a *first principles* deformation potential δV is used in combination with model wave functions. The model potential is calibrated to give the correct energy and wave function shape of the quantum-well state (final state $|f\rangle$) in comparison with experiment⁸ and a DFT calculation,²⁵ respectively. We are thus confident in describing the resonance states (initial states $|i\rangle$) deduced from the model potential. A fully self-consistent DFT calculation seems to us a difficult computational problem, illustrated by the present calculation, which requires a copper slab of thickness of about 100 Å in order to converge. In comparison with ARPES data, we show that the main contribution to the lifetime broadening of the quantum-well state of the system 1-ML Na on Cu(111) can be attributed to the electron-phonon coupling in the overlayer and interface region.

We want to thank V.P. Zhdanov and P. Apell for valuable comments on the manuscript and L. Bengtsson for help with the DACAPO computer code. This work has been supported by the Swedish Science Research Council. Economical support from Carl Tryggers Foundation is also acknowledged.

¹R. Landauer, J. Phys.: Condens. Matter **1**, 8099 (1989).

²D. Wharam, T.J. Thornton, R. Newbury, M. Pepper, H. Ahmed, J.E.F. Frost, D.G. Hasko, D.C. Peacock, D.A. Ritchie, and G.A.C. Jones, J. Phys. C **21**, L209 (1988).

³B. van Wees, H. van Houten, C.W.J. Beenakker, J.G. Williamson, D. van der Marel, and C.T. Foxton, Phys. Rev. Lett. **60**, 848 (1988).

⁴H. Benisty, Phys. Rev. B **51**, 13 281 (1995).

⁵M. Bäumer, M. Frank, S. Stempel, J. Libuda, and H.-J. Freund, Surf. Sci. **391**, 204 (1997).

⁶M. Frank, S. Andersson, J. Libuda, S. Stempel, A. Sandell, B.

Brena, A. Giertz, P.A. Brühwiler, M. Bäumer, N. Mårtensson, and H.-J. Freund, Chem. Phys. Lett. **297**, 92 (1997).

⁷E.V. Chulkov, I. Sarria, V.M. Silikin, J.M. Pitarke, and P. M. Echenique, Phys. Rev. Lett. **80**, 4947 (1998).

⁸A. Carlsson, B. Hellsing, S.-Å. Lindgren, and L. Walldén, Phys. Rev. B **56**, 1593 (1997).

⁹J.J. Paggel, T. Miller, and T.-C. Chiang, Phys. Rev. Lett. **81**, 5632 (1998).

¹⁰S.-Å. Lindgren and L. Walldén, Phys. Rev. Lett. **59**, 3003 (1987).

¹¹A. Carlsson, D. Claesson, S.-Å. Lindgren, and L. Walldén, Phys. Rev. Lett. **77**, 346 (1996).

- ¹²H. Petek, A.P. Heberle, W. Nessler, H. Nagano, S. Kubota, S. Matsunami, N. Moriya, and S. Ogawa, Phys. Rev. Lett. **79**, 4649 (1997).
- ¹³S. Ogawa, H. Nagano, and H. Petek, Phys. Rev. Lett. **79**, 4649 (1997).
- ¹⁴B. A. McDougall, T. Balasubramanian, and E. Jensen, Phys. Rev. B **51**, 13 891 (1995).
- ¹⁵A. Beckmann, Surf. Sci. **326**, 335 (1995).
- ¹⁶R. Matzdorf, Surf. Sci. Rep. **30**, 153 (1998).
- ¹⁷R. Matzdorf, G. Meister, and A. Goldmann, Surf. Sci. **286**, 56 (1993).
- ¹⁸M. Lee, Phys. Rev. B **2**, 250 (1970).
- ¹⁹G. Grimvall, in *The Electron-Phonon Interaction in Metals, Selected Topics in Solid State Physics*, edited by E. Wohlfarth (North-Holland, New York, 1981).
- ²⁰F. Khan, P. Allen, W. Butler, and F. Pinski, Phys. Rev. B **26**, 1538 (1982).
- ²¹J. Quinn, Phys. Rev. **126**, 1453 (1962).
- ²²G. Benedek, J. Ellis, A. Reichmuth, P. Ruggerone, H. Schief, and J.P. Toennies, Phys. Rev. Lett. **69**, 2951 (1992).
- ²³S.-Å. Lindgren and L. Walldén, Phys. Rev. B **38**, 3060 (1988).
- ²⁴N. Smith, N. Brookes, Y. Chang, and P. Johnson, Phys. Rev. B **49**, 332 (1994).
- ²⁵J. Carlsson and B. Hellsing (to be published).
- ²⁶P. Hohenberg and W. Kohn, Phys. Rev. **136**, A864 (1964).
- ²⁷W. Kohn and L. Sham, Phys. Rev. **140**, B1133 (1965).
- ²⁸J. Perdew, J. Chevary, S. Vosko, K. Jackson, M. Pederson, D. Singh, and C. Fiolhais, Phys. Rev. B **46**, 6671 (1992).
- ²⁹D. Vanderbilt, Phys. Rev. B **41**, 7892 (1990).
- ³⁰B. Hammer, K. Jacobsen, and J. Nørskov, Phys. Rev. Lett. **70**, 3971 (1993).
- ³¹L. Bengtsson, Ph.D. thesis, Chalmers University of Technology, Göteborg, Sweden, 1999.
- ³²S.-Å. Lindgren and L. Walldén, J. Electron Spectrosc. Relat. Phenom. **64/65**, 483 (1993).
- ³³B. Hellsing, Surf. Sci. **152/153**, 826 (1985).